Empirical description of β-delayed fission partial half-lives

L. Ghys,[1,2,*] A. N. Andreyev,[3,4] S. Antalic,[5] M. Huyse,[1] and P. Van Duppen[1]
[1]*KU Leuven, Instituut voor Kern- en Stralingsfysica, 3001 Leuven, Belgium*
[2]*Belgian Nuclear Research Centre SCK•CEN, Boeretang 200, B-2400 Mol, Belgium*
[3]*Department of Physics, University of York, York YO10 5DD, United Kingdom*
[4]*Advanced Science Research Center, Japan Atomic Energy Agency, Tokai-Mura, Naka-gun, Ibaraki 319-1195, Japan*
[5]*Department of Nuclear Physics and Biophysics, Comenius University, 84248 Bratislava, Slovakia*
(Received 30 January 2015; published 16 April 2015)

Background: The process of β-delayed fission (βDF) provides a versatile tool to study low-energy fission in nuclei far away from the β-stability line, especially for nuclei which do not fission spontaneously.
Purpose: The aim of this paper is to investigate systematic trends in βDF partial half-lives.
Method: A semi-phenomenological framework was developed to systematically account for the behavior of βDF partial half-lives.
Results: The βDF partial half-life appears to exponentially depend on the difference between the Q value for β decay of the parent nucleus and the fission-barrier energy of the daughter (after β decay) product. Such dependence was found to arise naturally from some simple theoretical considerations.
Conclusions: This systematic trend was confirmed for experimental βDF partial half-lives spanning over seven orders of magnitude when using fission barriers calculated from either the Thomas-Fermi or the liquid-drop fission model. The same dependence was also observed, although less pronounced, when comparing to fission barriers from the finite-range liquid-drop model or the Thomas-Fermi plus Strutinsky integral method.

DOI: 10.1103/PhysRevC.91.044314 PACS number(s): 24.75.+i, 23.40.−s, 21.10.Tg, 25.85.−w

I. INTRODUCTION

β-delayed fission (βDF) is a two-step process whereby the fissioning nucleus could be created in an excited state after β decay of a precursor. Since the excitation energy of the fissioning daughter product is limited by the Q_β value for β decay of the parent, βDF provides a unique tool to study low-energy fission of nuclei far from stability, especially for those not fissioning spontaneously. Figure 1 provides a schematic representation of this process, for nuclides on the neutron-deficient side of the nuclear chart. Recent experiments at ISOLDE-CERN [1–4] and SHIP-GSI [5,6] have studied this exotic decay mode in several short-lived neutron-deficient isotopes in the lead region. The fission-fragment mass and energy distributions resulting from βDF have established a new region of asymmetric fission around ^{178,180}Hg [1,3] and indicated multimodal fission in ^{194,196}Po and ^{202}Rn [4]. A recent review of the βDF process is given in Ref. [7], in which a total of 27 βDF cases, both on the neutron-rich and neutron-deficient sides, were summarized.

It is furthermore believed that βDF could, together with neutron-induced and spontaneous fission, influence the fission recycling in r-process nucleosynthesis [8,9]. Therefore, a reliable prediction of the relative importance of βDF in nuclear decay, often expressed by the βDF probability $P_{\beta\mathrm{DF}}$, is needed. $P_{\beta\mathrm{DF}}$ is defined as

$$P_{\beta\mathrm{DF}} = \frac{N_{\beta\mathrm{DF}}}{N_\beta}, \quad (1)$$

where $N_{\beta\mathrm{DF}}$ and N_β are respectively the number of βDF and β decays of the precursor nucleus. An earlier comparison of $P_{\beta\mathrm{DF}}$ data in a relatively narrow region of nuclei in the vicinity of uranium showed a simple exponential dependence with respect to Q_β [10,11]. It was assumed that fission-barrier heights B_f of the daughter nuclei do not vary greatly in this region [12] ($B_\mathrm{f} \sim 4$–6 MeV) and thus have a smaller influence on $P_{\beta\mathrm{DF}}$ as compared to Q_β values ($Q_\beta \sim 3$–6 MeV). In addition, these nuclei have a typical N/Z ratio around ∼1.4–1.5, which is close to that of traditional spontaneous fission of heavy actinides.

The aim of this paper is to further explore such systematic features by including the newly obtained data in the neutron-deficient lead region whose βDF nuclides have significantly different N/Z ratios (∼1.2–1.3), B_f (∼7–10 MeV), and Q_β values (∼9–11 MeV) as compared to those in the uranium region.

However, from an experimental point of view, the dominant α-branching ratio ($\gtrsim$90%) in most βDF precursors in the neutron-deficient lead region [13] makes precise determination of N_β in Eq. (1) difficult. Therefore, the partial βDF half-life $T_{1/2\mathrm{p},\beta\mathrm{DF}}$, as proposed in Ref. [7], is discussed in the present study. By analogy with other decay modes, $T_{1/2\mathrm{p},\beta\mathrm{DF}}$ is defined by

$$T_{1/2\mathrm{p},\beta\mathrm{DF}} = T_{1/2}\frac{N_{\mathrm{dec,tot}}}{N_{\beta\mathrm{DF}}}, \quad (2)$$

where $T_{1/2}$ represents the total half-life and $N_{\mathrm{dec,tot}}$ the number of decayed precursor nuclei. The relation between $T_{1/2\mathrm{p},\beta\mathrm{DF}}$ and $P_{\beta\mathrm{DF}}$ can be derived from Eqs. (1) and (2) as

$$T_{1/2\mathrm{p},\beta\mathrm{DF}} = \frac{T_{1/2}}{b_\beta P_{\beta\mathrm{DF}}}, \quad (3)$$

with b_β denoting the β-branching ratio. If the α-decay channel dominates, as is often the case in the neutron-deficient lead

*lars.ghys@fys.kuleuven.be

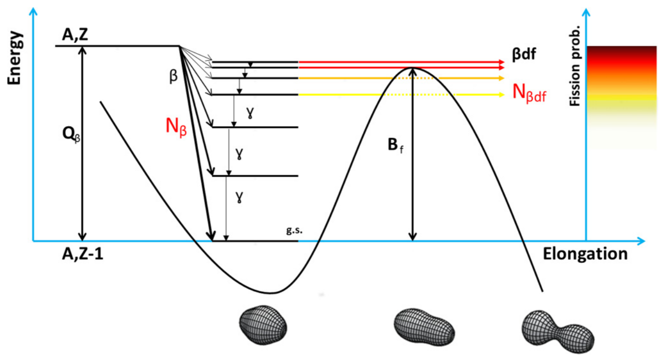

FIG. 1. (Color online) Schematic representation of the βDF process on the neutron-deficient side of the nuclear chart. The Q_{EC} value of the parent (A,Z) nucleus is indicated, while the curved line shows the potential energy of the daughter $(A,Z-1)$ nucleus with respect to nuclear elongation, displaying also the fission barrier B_f. The color code on the right-hand side represents the probability for excited states, with excitation energies close to B_f, to undergo fission; the darker colors correspond to higher probabilities.

region, one can safely approximate $N_{\rm dec,tot}$ in Eq. (2) by the amount of α decays, N_α.

This work shows an apparent exponential dependence of $T_{1/2{\rm p},\beta{\rm DF}}$ on $(Q_\beta - B_f)$ for certain sets of calculated fission-barrier energies. Such a relation may arise naturally by simple phenomenological approximations of the β-strength function of the precursor and the fission-decay width of excited states in the daughter nucleus. These assumptions may be justified considering the scale of the systematic trend discussed here, spanning $T_{1/2{\rm p},\beta{\rm DF}}$ values over several orders of magnitude. Deviations lower than one order of magnitude are thus acceptable.

II. THEORETICAL CONSIDERATIONS

Following Refs. [14–16], the expression for $P_{\beta{\rm DF}}$ is given by

$$P_{\beta{\rm DF}} = \frac{\int_0^{Q_\beta} S_\beta(E)F(Q_\beta - E)\frac{\Gamma_f(E)}{\Gamma_{\rm tot}(E)}dE}{\int_0^{Q_\beta} S_\beta(E)F(Q_\beta - E)dE}, \quad (4)$$

whereby the β-strength function of the parent nucleus is denoted by S_β and the Fermi function by F. The excitation energy is here, and further, given by E. The fission and total decay widths of the daughter, after β decay, are respectively given by Γ_f and $\Gamma_{\rm tot}$. Equation (3) can be combined with Eq. (4) to deduce the decay constant of βDF, defined as $\lambda_{\beta{\rm DF}} = \ln(2)/T_{1/2{\rm p},\beta{\rm DF}}$, as

$$\lambda_{\beta{\rm DF}} = \int_0^{Q_\beta} S_\beta(E)F(Q_\beta - E)\frac{\Gamma_f(E)}{\Gamma_{\rm tot}(E)}dE. \quad (5)$$

This section is devoted to the derivation of an analytical expression for $\lambda_{\beta{\rm DF}}$ by approximating S_β, F, and $\Gamma_f/\Gamma_{\rm tot}$. Since most of the reliable experimental data on βDF are recorded on the neutron-deficient side of the nuclear chart (see Table I and [7]), only fission preceded by electron capture (EC) or β^+ decay is considered here.

A. Approximations

A first simplification in Eq. (5) is to approximate S_β by a constant C_1, as proposed in previous studies (see for example Refs. [17,18]). Possible resonant structures in S_β, considered in, for example, Refs. [15,19], are thus ignored, thereby assuming a limited sensitivity of $T_{1/2{\rm p},\beta{\rm DF}}$ on S_β with respect to the scale of the systematic trend discussed here. This approximation is further supported by the study in Ref. [20], which shows a limited influence of S_β in the calculation of $P_{\beta{\rm DF}}$. Furthermore, C_1 was taken equal for all isotopes listed in Table I, thereby neglecting possible variations of C_1 with respect to the nuclear properties of the βDF precursors, such as mass, proton number, isospin, spin, and parity.

The Fermi function F can be fairly well described by the function $C_2(Q_{EC} - E)^2$ [21–23] for EC decay. The prefactor C_2 was again considered element independent, thereby ignoring its slight dependence on the atomic number Z [23]. According to Refs. [23,24], EC decay is dominant for transition energies below 5 MeV if Z exceeds 80. Since Q_β values of βDF precursors in the uranium region are typically smaller than 5 MeV (see Table I), β^+ decay can be disregarded here. Q_β values in the neutron-deficient lead region can, however, reach 10–11 MeV, implying a relatively high β^+ over EC decay ratio to the ground or a low-lying excited state in the daughter. However, since βDF should primarily happen at excitation energies which are only a few MeV below Q_β [25], EC-delayed fission should dominate over β^+-delayed fission in the full region of the nuclear chart (see later discussion).

The prompt decay of an excited state in a nucleus can, in the most general case, happen through fission, emission of a γ ray, proton, α particle, or neutron. The total decay width is thus given by $\Gamma_{\rm tot} = \Gamma_f + \Gamma_\gamma + \Gamma_p + \Gamma_\alpha + \Gamma_n$.

For the βDF precursors considered in Table I, the neutron separation energies exceed the Q_β value by at least several MeV [26] and charge particle emission is strongly hindered due to the large Coulomb barrier. Therefore, the deexcitation of states below Q_β is mostly dominated by γ decay, which makes that $\Gamma_{\rm tot} \simeq \Gamma_\gamma$ [20,27]. In addition, Γ_γ can be approximated by a constant (see for example Ref. [20]). Reference [27] provides a calculation of Γ_f with respect to the excitation energy E by including the fission-barrier penetrability and the influence of level densities at the ground state and saddle point. This calculation shows that Γ_f seems well approximated by a single exponential behavior $\Gamma_f \sim e^{-X(B_f - E)}$ at excitation energies around B_f. For the fissile nuclei listed in Table I, the decay constant adopts a value $X \approx 4$ MeV^{-1} [27]. The ratio $\Gamma_f/\Gamma_{\rm tot}$ is thus approximated by

$$\frac{\Gamma_f}{\Gamma_{\rm tot}}(E) \simeq \frac{\Gamma_f}{\Gamma_\gamma}(E) \approx C_3 e^{-X(B_f - E)}. \quad (6)$$

The constants C_3 and X are assumed to adopt the same value for all isotopes of interest. At excitation energies E moderately above B_f, deexcitation by fission should dominate and $\Gamma_f/\Gamma_{\rm tot}(E)$ will thus be close to unity. Since the Q_β value of most known βDF precursors (see Table I) does not exceed B_f of the daughter by more than a few MeV, it is further assumed that Eq. (6) remains valid for excitation energies in the daughter nucleus close to Q_β.

TABLE I. List of all precursors for which βDF was observed. The measured half-life $T_{1/2}$, β-branching ratio b_β, βDF probability $P_{\beta\mathrm{DF}}$, ratio of observed βDF to α decays $N_{\beta\mathrm{DF}}/N_\alpha$, and calculated βDF partial half-lives $T_{1/2\mathrm{p},\beta\mathrm{DF}}$ are listed. Reliable values for $T_{1/2\mathrm{p},\beta\mathrm{DF}}$, as evaluated by the criteria in Ref. [7], are indicated in bold. $(Q_\beta - B_\mathrm{f})$ is tabulated for fission barriers from four different fission models: the Thomas-Fermi (TF) model [30], the finite-range liquid-drop model (FRLDM) [31], the liquid-drop model (LDM) [27], and the extended Thomas-Fermi plus Strutinsky integral (ETFSI) model [28]. Q_β values were taken from Ref. [26] and are defined by Eq. (15).

Precursor	$T_{1/2}$ (s)	Q_β (MeV)	$Q_\beta - B_\mathrm{f}$ (MeV)				b_β	$P_{\beta\mathrm{DF}}$	$N_{\beta\mathrm{DF}}/N_\alpha$	$T_{1/2\mathrm{p},\beta\mathrm{DF}}$ (s)	Ref.
			TF	FRLDM	LDM	ETFSI					
				β^+/EC-delayed fission in the neutron-deficient lead region							
^{178}Tl	0.25(2)	11.5	2.5	2.2	3.0		0.38(2)	$1.5(6) \times 10^{-3}$		$\mathbf{4(2) \times 10^2}$	[3]
^{180}Tl	1.09(1)	11.0	1.4	1.2	2.6		0.94(4)	$3.2(2) \times 10^{-5}$		$\mathbf{3.6(3) \times 10^4}$	[2]
^{186g,m}Bi	0.012(3)[a]	11.6	2.8	2.0	3.1		∼0.006[b]		$2.2(13) \times 10^{-4}$	56(35)	[6]
^{188g,m}Bi	0.16(10)[a]	10.6	0.9	0.3	1.2		∼0.03[b]		$3.2(16) \times 10^{-5}$	$5(4) \times 10^3$	[6]
^{192g,m}At	0.05(4)[a]	11.0	4.2	2.8	4.2		∼0.03[b]		$4.2(9) \times 10^{-3}$	12(9)	[5]
^{194g,m}At	0.28(3)[a]	10.3	2.5	0.8	2.7		∼0.08[b]		$5.9(4) \times 10^{-5}$	$4.8(6) \times 10^2$	[4]
^{196}At	0.358(5)	9.6	0.3	− 0.7	1.1		0.026(1)	$9(1) \times 10^{-5}$	$2.3(2) \times 10^{-6}$	$\mathbf{1.5(2) \times 10^5}$	[4,34]
^{200}Fr	0.049(4)[a]	10.2	3.3	1.5	3.7		<0.021(4)	$>3.1(17) \times 10^{-2}$	$7^{+5}_{-3} \times 10^{-4}$	$\mathbf{7^{+6}_{-3} \times 10}$	[4]
^{202g,m}Fr	0.33(4)[c]	9.4	0.8	− 0.9	0.7		∼0.007[b]		$7.3(8) \times 10^{-7}$	$4.5(8) \times 10^4$	[4]
				β^+/EC-delayed fission in the neutron-deficient uranium region							
^{228}Np	61(1)	4.4	0.0	− 0.8	0.3		0.60(7)	$2.0(9) \times 10^{-4}$		$\mathbf{5.1(2) \times 10^5}$	[36]
^{232}Am	79(2)	4.9	1.3	1.7	0.5		∼0.96[b]	$6.9(10) \times 10^{-4}$		$\mathbf{1.2(2) \times 10^5}$	[37]
^{234}Am	139(5)	4.1	0.0	0.3	− 0.3	− 0.1	∼1.00[b]	$6.6(18) \times 10^{-5}$		$\mathbf{2.1(6) \times 10^6}$	[38]
^{238}Bk	144(5)	4.8	1.1	− 0.2	0.4	− 0.1	∼0.95[b]	$4.8(20) \times 10^{-4}$		$\mathbf{3.2(13) \times 10^5}$	[39]
^{240}Bk	252(48)	3.9	− 0.3	− 1.9	− 0.8	− 1.6	∼1.00[b]	$1.3^{+1.8}_{-0.7} \times 10^{-5}$		$\mathbf{1.9^{+2.3}_{-1.1} \times 10^7}$	[40]
^{242}Es	11(3)	5.4	1.8	− 0.7	1.2	− 0.1	0.57(3)[d]	$6(2) \times 10^{-3}$		$\mathbf{3(1) \times 10^3}$	[10]
^{244}Es	37(4)[a]	4.5	0.2	− 2.2	− 0.3	− 1.7	0.96(3)[e]	$1.2(4) \times 10^{-4}$		$\mathbf{3(1) \times 10^5}$	[11]
^{246}Es	462(30)	3.8	− 0.8	− 3.4	− 1.7	− 2.7	0.901(18)[e]	$3.7^{+8.5}_{-3.0} \times 10^{-5}$		$\mathbf{1.4^{+5.9}_{-1.0} \times 10^7}$	[42]
^{248}Es	$1.4(2) \times 10^3$	3.1	− 1.9	− 4.2	− 2.8	− 3.6	0.997(3)[e]	$3.5(18) \times 10^{-6}$		$\mathbf{4.0(21) \times 10^8}$	[42]
^{246m2}Md	4.4(8)	5.9	2.1	− 0.2	1.6	0.0	>0.77	>0.1		<57	[41]
^{250}Md	52(6)[a]	4.6	− 0.3	− 2.7	− 1.0	− 2.1	0.93(3)[e]	$2^{+2}_{-1} \times 10^{-4}$		$3^{+3}_{-1} \times 10^5$	[14]
				β^--delayed fission in the neutron-rich uranium region							
^{228}Ac	$2.214(7) \times 10^4$[a]	2.1	− 4.0	− 4.4	− 4.4	− 4.3	∼1.00[b]	$5(2) \times 10^{-12}$		$4(2) \times 10^{15}$	[43]
^{230}Ac	122(3)[a]	3.0	− 3.4	− 2.7	− 3.7	− 3.8	∼1.00[b]	$1.19(40) \times 10^{-9}$		$1.0(3) \times 10^{10}$	[44]
^{234g}Pa	$2.41(2) \times 10^4$[a]	2.2	− 3.4	− 2.7	− 3.8	− 2.6	∼1.00[b]	$3 \times 10^{-(12\pm1)}$		$8 \times 10^{(15\pm1)}$	[45]
^{234m}Pa	69.54(66)[a]	2.2	− 3.4	− 2.7	− 3.8	− 2.6	0.9984(4)	$10^{-(12\pm1)}$		$7 \times 10^{(13\pm1)}$	[45]
^{236}Pa	546(6)[a]	2.9	− 2.9	− 2.1	− 3.2	− 2.3	∼1.00[b]	$10^{-9\pm1}$		$5 \times 10^{(11\pm1)}$	[45]
^{238}Pa	138(6)[a]	3.6	− 2.3	− 2.0	− 3.2	− 2.1	∼1.00[b]	$<2.6 \times 10^{-8}$		$>5.3 \times 10^9$	[46]
^{256m}Es	2.7×10^4[a]	1.7	− 2.3	− 3.4	− 3.2	− 3.8	∼1.00[b]	$\sim 2 \times 10^{-5}$		$\sim 1 \times 10^9$	[47]

[a]Value extracted according to Eq. (16) by using evaluated experimental data from Ref. [13].
[b]Calculated β-branching ratio from Ref. [33].
[c]Value extracted according to Eq. (16) by using experimental data from Ref. [35].
[d]β-branching ratio from Ref. [41].
[e]Evaluated β-branching ratio from Ref. [13].

Using the above approximations and taking $C = C_1 C_2 C_3$, the right-hand side of Eq. (5) reduces to

$$\lambda_{\beta\mathrm{DF}} = C \int_0^{Q_\beta} (Q_\beta - E)^2 e^{-X(B_\mathrm{f} - E)} dE. \qquad (7)$$

B. Calculating λ_{bdf}

Equation (7) can be rewritten, in order to isolate the exponential dependance on $(Q_\beta - B_\mathrm{f})$, as

$$\lambda_{\beta\mathrm{DF}} = C e^{X(Q_\beta - B_\mathrm{f})} \int_0^{Q_\beta} (Q_\beta - E)^2 e^{-X(Q_\beta - E)} dE. \qquad (8)$$

The integrand in Eq. (8) is thus proportional to the βDF probability at a given E of the daughter nucleus. This function, plotted in Fig. 2 for different values of X around the deduced value $X \approx 4\ \mathrm{MeV}^{-1}$ from Ref. [27], shows that βDF primarily happens at energy levels 0–2 MeV below Q_β. Moreover, since all Q_β values of the neutron-deficient βDF precursors listed in Table I exceed ∼2 MeV, the value of the integral in Eq. (8) is little dependent on the precise value of Q_β. As a consequence, $\lambda_{\beta\mathrm{DF}}$ primarily depends on the difference $(Q_\beta - B_\mathrm{f})$.

In order to prove the latter statement analytically, a substitution with $u = X(Q_\beta - E)$ and adjustment of integration borders in Eq. (8) is performed:

$$\lambda_{\beta\mathrm{DF}} = \frac{C e^{X(Q_\beta - B_\mathrm{f})}}{X^3} \int_0^{XQ_\beta} u^2 e^{-u} du. \qquad (9)$$

The integral in Eq. (9) is similar to the mathematical form of the so-called normalized upper incomplete Γ function, defined

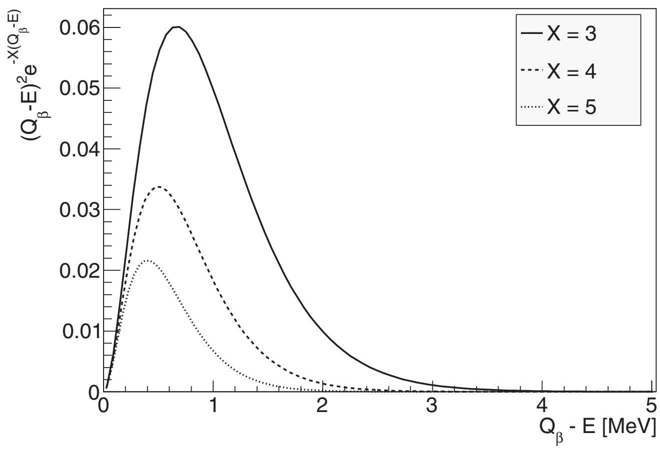

FIG. 2. Plot showing the integrand of Eq. (8), which is proportional to the βDF probability, for X equal to 3, 4, or 5.

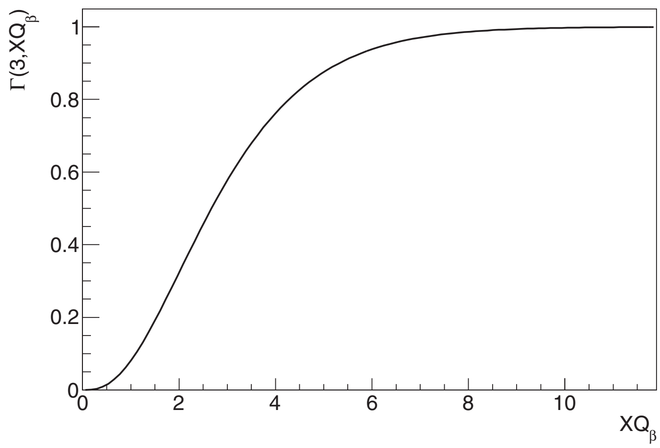

FIG. 3. The normalized incomplete Γ function $\Gamma(3,XQ_\beta)$, needed for the calculation of the integral under the βDF probability curves shown in Fig. 2.

as

$$\Gamma(s,x) = \frac{1}{\Gamma(s)}\int_0^x t^{s-1}e^{-t}dt, \tag{10}$$

whereby $\Gamma(s)$ is

$$\Gamma(s) = \int_0^{+\infty} t^{s-1}e^{-t}dt. \tag{11}$$

Equation (9) thus transforms into

$$\lambda_{\beta\mathrm{DF}} = \frac{Ce^{X(Q_\beta - B_\mathrm{f})}}{X^3}\Gamma(3)\Gamma(3,XQ_\beta). \tag{12}$$

Table I shows that all Q_β values of the neutron-deficient βDF precursors exceed 3 MeV, while the fitted values for X in Table II, as well as the theoretical estimate from Ref. [27] ($X \approx 4$ MeV^{-1}), are all greater than 1.7 MeV^{-1}. The value XQ_β thus exceeds 5 in all discussed cases, implying that, as shown in Fig. 3, one can thus safely approximate $\Gamma(3,XQ_\beta) \simeq 1$ in Eq. (12).

In this simple picture, it is thus found that $\ln(\lambda_{\beta\mathrm{DF}})$ depends linearly on $(Q_\beta - B_\mathrm{f})$. In terms of the partial βDF half-life $T_{1/2\mathrm{p},\beta\mathrm{DF}}$ one finds the relation

$$\log_{10}(T_{1/2\mathrm{p},\beta\mathrm{DF}}) = C' - X\log_{10}(e)(Q_\beta - B_\mathrm{f}), \tag{13}$$

TABLE II. Results of the fits, corresponding to four different fission models, shown in Fig. 4. The values for the parameters X and C' in Eq. (13) are listed. Also the root-mean-square deviations (RMSDs) of the reliable experimental $\log_{10}(T_{1/2\mathrm{p},\beta\mathrm{DF}})$ values (represented by the closed symbols in Fig. 4) to the fit are given.

Model	X (MeV^{-1})	C' (MeV)	RMSD
TF	3.0(2)	6.2(1)	0.47
FRLDM	1.7(4)	4.9(3)	1.19
ETFSI	2.1(7)	5.0(6)	1.10
LDM	2.2(2)	5.8(2)	0.62

with the constant C' given by

$$C' = \ln\left(\frac{\ln(2)X^3}{C\Gamma(3)}\right)\log_{10}(e). \tag{14}$$

III. SYSTEMATIC COMPARISON OF EXPERIMENTAL DATA

This section aims at verifying Eq. (13) by using experimental βDF partial half-lives and theoretical values for $(Q_\beta - B_\mathrm{f})$, summarized in Table I and Fig. 4. Tabulated fission barriers from four different fission models were used, of which three are based on a macroscopic-microscopic and one a mean-field approach. The latter model is based on the extended Thomas-Fermi plus Strutinsky integral (ETFSI) method [28], but tabulated barriers for the most neutron-deficient isotopes in Table I are absent from the literature. The microscopic-macroscopic approaches all rely on shell corrections from Ref. [29] and describe the macroscopic structure of the nucleus by either a Thomas-Fermi (TF) model [30], liquid-drop model (LDM) [27] or the finite-range liquid-drop model (FRLDM) [31]. The Q_β values were taken from the 2012 atomic mass evaluation tables [26] and are derived from the difference between the atomic masses of parent $M_P(Z,A)$ and daughter $M_D(Z',A)$ nuclei as

$$Q_\beta = c^2[M_P(Z,A) - M_D(Z',A)]. \tag{15}$$

About half of these values are known from experiments, while the others are deduced from extrapolated atomic masses. In latter cases, the difference of the Q_β values from Ref. [26] with the theoretical values from Refs. [29] or [32] is always lower than 0.4 MeV.

$T_{1/2\mathrm{p},\beta\mathrm{DF}}$ values were extracted from reported $P_{\beta\mathrm{DF}}$ values using Eq. (3), if the precursor nucleus has a significant β-decay branch ($b_\beta \gtrsim 10\%$). When multiple measurements on $P_{\beta\mathrm{DF}}$ were performed, only the reliable value, as evaluated by Ref. [7], or the most recent value was tabulated. In case of a dominant α-decay branch ($b_\beta \lesssim 10\%$), $T_{1/2\mathrm{p},\beta\mathrm{DF}}$ was calculated by Eq. (2), whereby $N_{\mathrm{dec,tot}}$ was approximated by

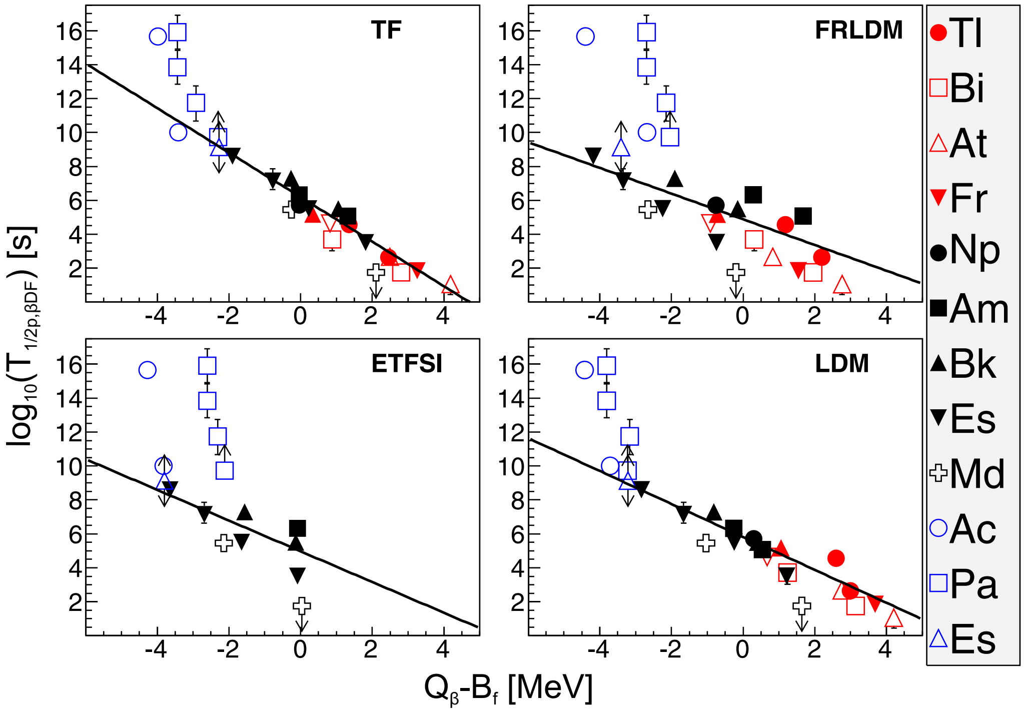

FIG. 4. (Color online) Plots of $T_{1/2p,\beta DF}$ versus $(Q_\beta - B_f)$ for different fission models as listed in Table I. The solid symbols, representing reliable values for $T_{1/2p,\beta DF}$ in Table I, are used for a linear fit with equal weights to the data points. Other data from Table I are indicated by the open symbols. The color code represents the different regions of the nuclear chart for which βDF has been experimentally observed: the neutron-deficient lead region (red), and the neutron-deficient (black) and neutron-rich (blue) uranium regions.

the observed amount of α decays, N_α, corrected for detection efficiency.

Since the isotopes ^{186,188}Bi, ^{192,194}At, and ^{202}Fr have both a ground and a low-lying α-decaying isomeric state with comparable half-lives, only an overall $N_{\beta DF}/N_\alpha$ value could be extracted with present experimental techniques. We refer the reader for a detailed discussion of this issue to Refs. [4–6]. Therefore, these precursors have been excluded from the fit in Fig. 4. Nonetheless, as a first approximation the value for $T_{1/2p,\beta DF}$ was extracted by defining the half-life $T_{1/2}$, shown in Table I, as the unweighted average

$$T_{1/2} = \frac{T_{1/2,g} + T_{1/2,m}}{2}, \tag{16}$$

where the respective half-lives for ground and isomeric states are denoted by $T_{1/2,g}$ and $T_{1/2,m}$. The uncertainty $\Delta T_{1/2}$ is conservatively taken as

$$\Delta T_{1/2} = \frac{|T_{1/2,g} - T_{1/2,m}|}{2}. \tag{17}$$

Figure 4 shows $\log_{10}(T_{1/2p,\beta DF})$ against $(Q_\beta - B_f)$ for the fission barriers from the four different models under consideration. Using the same evaluation criteria as proposed in Ref. [7] for $P_{\beta DF}$ measurements, 13 reliable $T_{1/2p,\beta DF}$ values, marked in bold in Table I, were selected. These data points, represented by the solid symbols, are fitted by a linear function. An equal weight to all fit points is given because the experimental uncertainties on $\log_{10}(T_{1/2p,\beta DF})$ are in most cases much smaller than the deviation of the data points with the fitted line, of which the extracted parameters are summarized in Table II. The remaining data points from Table I are shown by open symbols and were excluded from the fit. The color code discriminates between the neutron-deficient lead region (red), and the neutron-deficient (black) and neutron-rich (blue) uranium regions.

Figure 4 illustrates a linear dependence of $\log_{10}(T_{1/2p,\beta DF})$ on $(Q_\beta - B_f)$ for TF and LDM barriers for over seven orders of magnitude of $T_{1/2p,\beta DF}$. In addition, Table II shows a relatively small root-mean-square deviation (RMSD) of the 13 reliable experimental $\log_{10}(T_{1/2p,\beta DF})$ values (represented by the solid symbols in Fig. 4) to the corresponding values extracted from the fit. The dependence is somewhat less pronounced for the FRLDM, as evidenced by a larger RMSD value. A similar linear trend is observed for the ETFSI model, but the lack of tabulated fission barriers in the neutron-deficient region, especially in the lead region, prohibits drawing definite conclusions.

Moreover, Table II shows that the four fitted values for X are similar to each other as well as to the theoretical estimate $X \approx 4\ \text{MeV}^{-1}$ [27]. The extracted values for the offset C' are also found to be comparable.

In contrast to a rather good agreement for most neutron-deficient nuclei, all models show a larger systematical deviation from this linear trend for the neutron-rich βDF precursors ^{228}Ac and ^{234,236}Pa. In Ref. [7], concerns were raised on the accuracy of the $P_{\beta DF}$ values measured in this region, which could explain this deviation. Note also that the precursors in this region of the nuclear chart undergo β^- decay in contrast to the EC-delayed fission on the neutron-deficient side for which Eq. (13) was deduced, influencing the numeric value of the offset C'. In particular, the Fermi function for β^- decay is approximately proportional to $(Q_\beta - E)^5$ [16,22], in contrast to the quadratic dependence on $(Q_\beta - E)$ for EC decay. The parameter X should, however, remain unchanged, because Eq. (6) approximating Γ_f/Γ_{tot} remains valid as long as the neutron-separation energy S_n is larger than Q_β. At excitation energies higher than S_n, deexcitation through neutron emission is favored over decay by γ-ray emission, thus implying $\Gamma_{tot} \simeq \Gamma_n \gg \Gamma_\gamma, \Gamma_f$ [27,48]. For all nuclei mentioned in Table I, however, Q_β is below S_n. An approximation of $T_{1/2p,\beta DF}$, similar to Eq. (13), can thus also be derived for neutron-rich βDF precursors by taking into account the above considerations. However, considering the limited experimental information on βDF in the neutron-rich region, a detailed derivation is omitted in this paper.

IV. CONCLUSIONS

Recent experiments have measured the βDF of nine precursor nuclei in the neutron-deficient lead region. Because of the dominant α-decay branch in most of these nuclei, βDF probabilities are extracted with large experimental uncertainties. In contrast, the partial half-life for βDF can be determined with a better accuracy. In addition, $T_{1/2p,\beta DF}$ can be easily derived from the βDF probability by using Eq. (3).

A systematical evaluation of βDF partial half-lives was performed by using fission barriers deduced from four different models for a broad range of nuclei in the lead and uranium regions. A linear relation between $\log_{10}(T_{1/2p,\beta DF})$ and $(Q_\beta - B_f)$ was observed for neutron-deficient precursor nuclei when using tabulated fission barriers from the TF or LDM approach, and to a lesser extent for FRLDM and ETFSI barriers. This linear trend persists for values of $T_{1/2p,\beta DF}$ spanning over seven orders of magnitude and a wide variety of precursor nuclei going from ^{178}Tl to ^{248}Es with N/Z ratios of 1.20 and 1.51, respectively. This observation may help to assess βDF branching ratios in very neutron-rich nuclei, which are inaccessible by present experimental techniques but might play a role in the fission-recycling mechanism of the r-process nucleosynthesis.

ACKNOWLEDGMENTS

This work has been funded by FWO-Vlaanderen (Belgium), by the Slovak Research and Development Agency (Contract No. APVV-0105-10), by the UK Science and Technology Facilities Council (STFC), by the Slovak grant agency VEGA (Contract No. 1/0576/13), by the Reimei Foundation of JAEA, and by the European Commission within the Seventh Framework Programme through I3-ENSAR (Contract No. RII3-CT-2010-262010).

[1] A. N. Andreyev *et al.*, Phys. Rev. Lett. **105**, 252502 (2010).
[2] J. Elseviers *et al.*, Phys. Rev. C **88**, 044321 (2013).
[3] V. Liberati *et al.*, Phys. Rev. C **88**, 044322 (2013).
[4] L. Ghys *et al.*, Phys. Rev. C **90**, 041301 (2014).
[5] A. N. Andreyev *et al.*, Phys. Rev. C **87**, 014317 (2013).
[6] J. F. W. Lane *et al.*, Phys. Rev. C **87**, 014318 (2013).
[7] A. N. Andreyev, M. Huyse, and P. Van Duppen, Rev. Mod. Phys. **85**, 1541 (2013).
[8] I. V. Panov, E. Kolbe, B. Pfeiffer, T. Rauscher, K.-L. Kratz, and F.-K. Thielemann, Nucl. Phys. A **747**, 633 (2005).
[9] I. Petermann, K. Langanke, G. Martínez-Pinedo, I. V. Panov, P. G. Reinhard, and F. K. Thielemann, Eur. Phys. J. A **48**, 122 (2012).
[10] D. A. Shaughnessy, J. L. Adams, K. E. Gregorich, M. R. Lane, C. A. Laue, D. M. Lee, C. A. McGrath, J. B. Patin, D. A. Strellis, E. R. Sylwester, P. A. Wilk, and D. C. Hoffman, Phys. Rev. C **61**, 044609 (2000).
[11] D. A. Shaughnessy, K. E. Gregorich, J. L. Adams, M. R. Lane, C. A. Laue, D. M. Lee, C. A. McGrath, V. Ninov, J. B. Patin, D. A. Strellis, E. R. Sylwester, P. A. Wilk, and D. C. Hoffman, Phys. Rev. C **65**, 024612 (2002).
[12] H. C. Britt, E. Cheifetz, D. C. Hoffman, J. B. Wilhelmy, R. J. Dupzyk, and R. W. Lougheed, Phys. Rev. C **21**, 761 (1980).
[13] G. Audi, F. G. Kondev, M. Wang, B. Pfeiffer, X. Sun, J. Blachot, and M. MacCormick, Chin. Phys. C **36**, 1157 (2012).
[14] Y. P. Gangrsky, M. B. Miller, L. V. Mikhailov, and I. F. Kharisov, Sov. J. Nucl. Phys. **31**, 162 (1980).
[15] H. V. Klapdor, Prog. Part. Nucl. Phys. **10**, 131 (1983).
[16] V. I. Kuznetsov and N. K. Skobelev, Phys. Part. Nucl. **30**, 666 (1999).
[17] K. L. Kratz and G. Herrmann, Z. Phys. **263**, 435 (1973).
[18] P. Hornshoj, B. R. Erdal, P. G. Hansen, B. Jonson, K. Aleklett, and G. Nyman, Nucl. Phys. A **239**, 15 (1974).
[19] I. N. Izosimov, V. G. Kalinnikov, and A. A. Solnyshkin, Phys. Part. Nucl. **42**, 963 (2011).
[20] M. Veselský, A. N. Andreyev, S. Antalic, M. Huyse, P. Möller, K. Nishio, A. J. Sierk, P. Van Duppen, and M. Venhart, Phys. Rev. C **86**, 024308 (2012).
[21] D. Habs, H. Klewe-Nebenius, V. Metag, B. Neumann, and H. J. Specht, Z. Phys. **285**, 53 (1978).
[22] H. L. Hall and D. C. Hoffman, Annu. Rev. Nucl. Part. Sci. **42**, 147 (1992).
[23] M. Emeric and A. Sonzogni, http://www.nndc.bnl.gov/logft/
[24] R. B. Firestone, in *Table of Isotopes*, 8th ed., edited by V. S. Shirley (Wiley, New York, 1999), pp. 14188–14192.
[25] P. Möller, J. Randrup, and A. J. Sierk, Phys. Rev. C **85**, 024306 (2012).
[26] M. Wang, G. Audi, A. H. Wapstra, F. G. Kondev, M. MacCormick, X. Xu, and B. Pfeiffer, Chin. Phys. C **36**, 1603 (2012).
[27] V. Zagrebaev, A. Denikin, A. P. Alekseev, A. V. Karpov, V. V. Samarin, M. A. Naumenko, and A. Y. Kozhin, http://nrv.jinr.ru/nrv/
[28] A. Mamdouh, J. M. Pearson, M. Rayet, and F. Tondeur, Nucl. Phys. A **679**, 337 (2001).
[29] P. Möller, J. R. Nix, W. D. Myers, and W. J. Swiatecki, At. Data Nucl. Data Tables **59**, 185 (1995).
[30] W. D. Myers and W. J. Światecki, Phys. Rev. C **60**, 014606 (1999).
[31] P. Möller, A. J. Sierk, T. Ichikawa, A. Iwamoto, and M. Mumpower, Phys. Rev. C **91**, 024310 (2015).

[32] W. D. Myers and W. J. Swiatecki, Nucl. Phys. A **601**, 141 (1996).
[33] P. Möller, J. R. Nix, and K.-L. Kratz, At. Data Nucl. Data Tables **66**, 131 (1997).
[34] V. L. Truesdale, A. N. Andreyev, B. Andel, S. Antalic, A. Barzakh, L. Capponi, T. E. Cocolios, X. Derkx, H. De Witte, J. Elseviers, D. V. Fedorov, V. N. Fedosseev, F. P. Hessberger, L. Ghys, M. Huyse, Z. Kalaninova, U. Köster, J. F. W. Lane, V. Liberati *et al.* (unpublished).
[35] Z. Kalaninová, S. Antalic, A. N. Andreyev, F. P. Hessberger, D. Ackermann, B. Andel, L. Bianco, S. Hofmann, M. Huyse, B. Kindler, B. Lommel, R. Mann, R. D. Page, P. J. Sapple, J. Thomson, P. Van Duppen, and M. Venhart, Phys. Rev. C **89**, 054312 (2014).
[36] S. A. Kreek, H. L. Hall, K. E. Gregorich, R. A. Henderson, J. D. Leyba, K. R. Czerwinski, B. Kadkhodayan, M. P. Neu, C. D. Kacher, T. M. Hamilton, M. R. Lane, E. R. Sylwester, A. Türler, D. M. Lee, M. J. Nurmia, and D. C. Hoffman, Phys. Rev. C **50**, 2288 (1994).
[37] H. L. Hall, K. E. Gregorich, R. A. Henderson, C. M. Gannett, R. B. Chadwick, J. D. Leyba, K. R. Czerwinski, B. Kadkhodayan, S. A. Kreek, N. J. Hannink, D. M. Lee, M. J. Nurmia, D. C. Hoffman, C. E. A. Palmer, and P. A. Baisden, Phys. Rev. C **42**, 1480 (1990).
[38] H. L. Hall, K. E. Gregorich, R. A. Henderson, C. M. Gannett, R. B. Chadwick, J. D. Leyba, K. R. Czerwinski, B. Kadkhodayan, S. A. Kreek, D. M. Lee, M. J. Nurmia, D. C. Hoffman, C. E. A. Palmer, and P. A. Baisden, Phys. Rev. C **41**, 618 (1990).
[39] S. A. Kreek, H. L. Hall, K. E. Gregorich, R. A. Henderson, J. D. Leyba, K. R. Czerwinski, B. Kadkhodayan, M. P. Neu, C. D. Kacher, T. M. Hamilton, M. R. Lane, E. R. Sylwester, A. Türler, D. M. Lee, M. J. Nurmia, and D. C. Hoffman, Phys. Rev. C **49**, 1859 (1994).
[40] D. Galeriu, J. Phys. G: Nucl. Phys. **9**, 309 (1983).
[41] S. Antalic, F. P. Hessberger, S. Hofmann, D. Ackermann, S. Heinz, B. Kindler, I. Kojouharov, P. Kuusiniemi, M. Leino, B. Lommel, R. Mann, and Š. Šáro, Eur. Phys. J. A **43**, 35 (2010).
[42] D. A. Shaughnessy, K. E. Gregorich, M. R. Lane, C. A. Laue, D. M. Lee, C. A. McGrath, D. A. Strellis, E. R. Sylwester, P. A. Wilk, and D. C. Hoffman, Phys. Rev. C **63**, 037603 (2001).
[43] X. Yanbing, Z. Shengdong, D. Huajie, Y. Shuanggui, Y. Weifan, N. Yanning, L. Xiting, Li Yingjun, and X. Yonghou, Phys. Rev. C **74**, 047303 (2006).
[44] Y. Shuanggui, Y. Weifan, X. Yanbing, P. Qiangyan, X. Bing, H. Jianjun, W. Dong, L. Yingjun, M. Taotao, and Y. Zhenguo, Eur. Phys. J. A **10**, 1 (2001).
[45] Y. P. Gangrsky, G. M. Marinesky, M. B. Miller, V. N. Samsuk, and I. F. Kharisov, Yad. Fiz. **27**, 894 (1978) [Sov. J. Nucl. Phys. **27**, 475 (1978)].
[46] A. Baas-May, J. V. Kratz, and N. Trautmann, Z. Phys. A: At. Nucl. **322**, 457 (1985).
[47] H. L. Hall, K. E. Gregorich, R. A. Henderson, D. M. Lee, D. C. Hoffman, M. E. Bunker, M. M. Fowler, P. Lysaght, J. W. Starner, and J. B. Wilhelmy, Phys. Rev. C **39**, 1866 (1989).
[48] N. Bohr and J. A. Wheeler, Phys. Rev. **56**, 426 (1939).